Applied Physics B (2018) 124:81
https://doi.org/10.1007/s00340-018-6948-3

Applied Physics B
Lasers and Optics

Frequency-dependent absorbance of broadband terahertz wave in dense plasma sheet

Yan Peng[1] · Binbin Qi[1] · Xiankai Jiang[1] · Zhi Zhu[1] · Hongwei Zhao[2] · Yiming Zhu[1]

Received: 14 August 2017 / Accepted: 9 April 2018 / Published online: 19 April 2018

Abstract
Due to the ability of accurate fingerprinting and low-ionization for different substances, terahertz (THz) technology has a lot of crucial applications in material analysis, information transfer, and safety inspection, etc. However, the spectral characteristic of atmospheric gas and ionized gas has not been widely investigated, which is important for the remote sensing application. Here, in this paper, we investigate the absorbance of broadband terahertz wave in dense plasma sheet generated by femtosecond laser pulses. It was found that as the terahertz wave transmits through the plasma sheet formed, respectively, in carbon dioxide, oxygen, argon and nitrogen, spectrum presents completely different and frequency-dependent absorbance. The reasons for these absorption peaks are related to the molecular polarity, electric charge, intermolecular and intramolecular interactions, and collisional absorption of gas molecules. These results have significant implications for the remote sensing of gas medium.

1 Introduction

Detecting and analyzing the components of atmosphere at remote location is an important subject for its widely application in greenhouse gas monitoring, examination of air pollution, meteorological observations, free-space optical communication, and so on. The unique capabilities—propagating unchanged over a few 100 m distances, and the easy tunability of the position of filamentation in space—make the laser-induced filaments become one of the most effective means for remote sensing [1–3]. Miguel Rodriguez et al. reported that they have observed the filamentation occurs up to 2 km altitude pumped by femtosecond-terawatt laser pulses (100 fs, the peak power of 3 TW in the near infrared, at a repetition of 10 Hz), showing the evidence for remote nonlinear propagation of high-power ultrashort laser pulses in atmosphere [1].

At the same time, as one kind of effective sensing and imaging technologies, terahertz (THz) spectroscopy has been widely used for characterizing the electronic, vibrational and compositional properties of solid, liquid and gas phase materials [4–6]. For example, in the year of 2003, Jamison et al. have measured the properties of a He-discharge plasma such as density and collisional frequency through terahertz time-domain spectroscopy methods. In this way, they solved the problem that laser and microwave measurements require different frequencies to unambiguously determine the phase change of low-density plasma [5].

Here, in this paper, we propose one effective remote sensing method to detect and distinguish gas by combining the laser filament and THz wave. Here, we choose CO_2, O_2, Ar and N_2 as examples, which are the basic components of atmosphere and including the monatomic gas, diatomic molecule and triatomic molecule. Additionally, the further qualitatively study is meaningful for the recognition of the gas composition and then remote sensing [7–11].

2 Experiments

In the experiments, laser pulses were produced by a Ti: Sapphire regenerative amplifier, typically 7.5 mJ laser pulses with a 130 fs temporal length, 800 nm mean wavelength and 1 kHz repetition rate. The output laser beam was split into three parts (6:3:1), which were used as plasma sheet

✉ Yiming Zhu
ymzhu@usst.edu.cn

[1] Shanghai Key Lab of Modern Optical System, University of Shanghai for Science and Technology, No. 516, Jungong Road, Shanghai 200093, China

[2] Shanghai Institute of Applied Physics, Chinese Academy of Sciences, Shanghai 201800, China

generation (part 1), THz wave generation (part 2) and THz EO detection (part 3), respectively.

The part 1 was used as the pump source for plasma sheet formation. The laser beam was focused by two uniaxial cylindrical lenses, as shown in Fig. 1a, whose focal lengths are 1000 and 200 mm in the *Y*- and *X*-direction, respectively. Based on the pump energy and beam-focusing condition discussed above, a strong-field tunneling ionization was expected to dominate (the variation range of the plasma intensity was 7×10^{13}–5×10^{14} W/cm^2) [12, 13]. Therefore, the gas medium around the expected plasma position was well ionized and one bright plasma can be clearly observed with the length of 10 mm. Considering the uniaxial cylindrical lens can only focus the laser beam in one dimension (*X* or *Y* dimension), therefore, plasma sheet could be formed effectively when the two cylindrical lenses have different distances away from the expected plasma position as compared to their focal lengths (i.e., the laser beam have different spot sizes in *X* and *Y* dimensions). In our experiments, the distances of these two cylindrical lenses away from the expected plasma sheet position were set as 900 and 200 mm, respectively. As a result, the cross section of plasma sheet should be lengthwise ellipse (in the *XY* plane). To show this picture directly, we reduced the power of laser beam and used a CMOS camera (LaserCam-HR) to record the cross section of plasma sheet at the center of filament [see Fig. 1b], whose size was 200 and 1000 μm in the *X* and *Y* dimensions, respectively. However, we must notice that this CCD image was recorded under very weak laser power, which can just show the shape of cross section of plasma sheet, but not the real size under the nonlinear filament case, especially the thickness of plasma sheet (in *X* dimension). Therefore, using a CCD camera (DS-CBY501-H), we took the photo of the top view of the plasma sheet to clear its thickness [see Fig. 1c], where the corresponding size was 250 μm. Combing all of these, the final length, width and thickness of the plasma sheet was determined as $10\times1\times0.25$ mm.

The part 2 was used as the pump source for terahertz wave generation via a two-color filament in air [11, 12, 14–18]. The terahertz radiations emitted from the filament were collected and then focused again to pass through the center of plasma sheet at a normal incidence, where the focal radius was ~0.36 mm. The interaction region of plasma sheet and THz wave was enclosed in a chamber, where pure gas (99.999%) was introduced with pressure kept at 1 atm. The windows of chamber for the two corresponding beams were 30-mm-diameter high transmittance at 800 nm and Teflon plates, respectively. Considering the transmissions of windows and plasma sheet, the signal-to-noise ratio of THz signal, the effective spectral range of our system is limited to 0.4–2.6 THz.

The part 3 was used as the probe light for the electro-optic sampling (EOS) detection of THz pulses with a 1 mm-thick (110) ZnTe crystal. To reduce the impact of water vapor for signal detection, the whole experimental system was enclosed in a big chamber purged with clean dry air (humidity < 3%).

It has been known that the ionization process of gas medium caused by femtosecond laser pulse is related to the

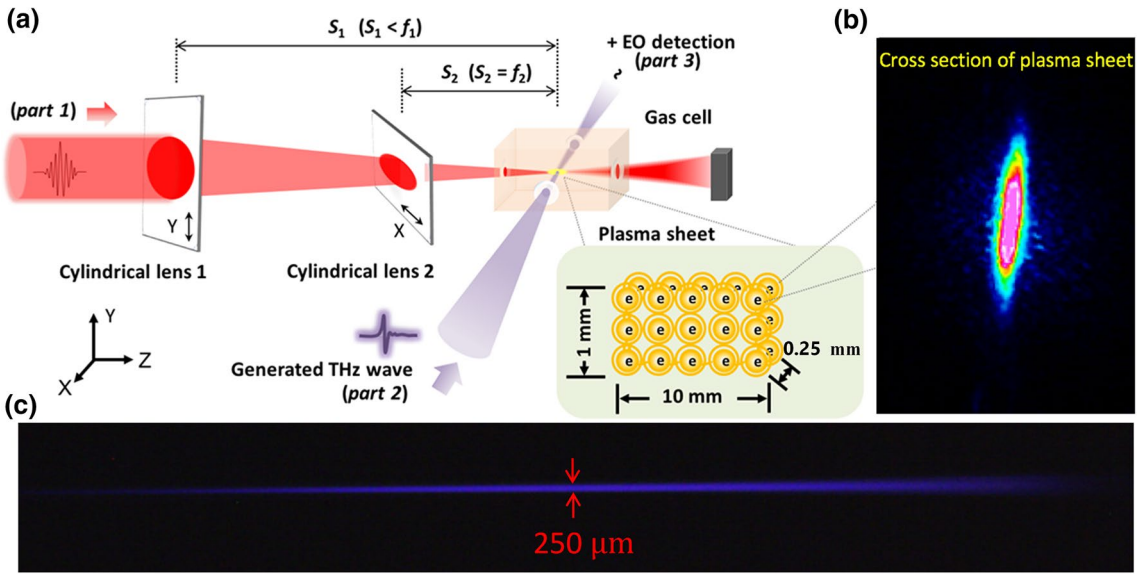

Fig. 1 **a** The schematic of interaction between terahertz wave and plasma sheet. $S_1 = 900$ mm, $f_1 = 1000$ mm, $S_2 = 200$ mm, $f_2 = 200$ mm. **b** The cross section of plasma sheet, which was measured by a CMOS camera (LaserCam-HR). **c** The top view of plasma sheet, which was measured by a CCD camera (DS-CBY501-H)

Gaussian distribution of pulse, and the corresponding refractive index of formed plasma changes fast. When the plasma is formed by femtosecond laser pulses, it will experience the process of generation, stable existence, vanish, where the entire process will last for about hundreds picosecond. To ensure the stability of the interaction between plasma sheet and THz beam, the meet moment between plasma and THz wave should locate during the "stable existence" stage of plasma sheet. Therefore, we chose the moment that the THz wave was about 27 ps later than that of the plasma generation, as the arrow shown in Fig. 2. After the experimental chamber was filled by pure gas and the plasma accepted a sufficiently long optical pumping, we detected and recorded THz waveforms by changing the delay in probe beam.

3 Results and discussion

In the experiments, the absorbance A is defined as $A = \log(\Phi_{Ref}/\Phi_{tra})$, with Φ_{Ref} and Φ_{tra} are the reference signal and transmitted signal, respectively, i.e., the detected THz wave without and with the function of the plasma sheet.

As shown in Fig. 3, for plasma sheet formed in different gas mediums, the transmitted THz spectra present different absorption peaks and different relative amplitudes obviously. According to the fingerprint spectrum characteristic of THz wave, these different THz absorption peaks indicate that there exist different molecules, radicals and interactions between them. These results also prove that different gas plasmas can be distinguished effectively by THz spectra. Thereby, in turn, we can deduce the composition of unknown substance based on those known THz spectrum

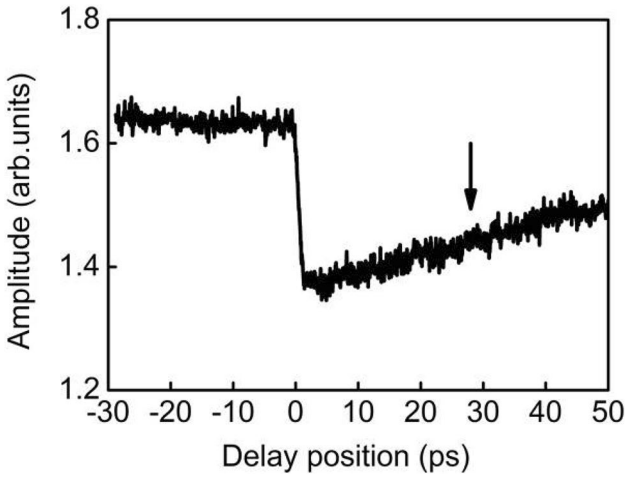

Fig. 2 THz amplitude as a function of delay between plasma and THz wave. The black arrow is the position of the THz wave relative to the plasma in the whole experiments

characteristics, which can be further applied in the remote sensing of gas composition.

Considering the plasma sheets are composed of mixtures of atoms, molecules, ions and electrons (see Table 1), the THz absorption peaks in each spectrum may be contributed by many reasons, therefore, we list the related factors of THz absorption spectra and give the qualitative analysis:

1. Rotational spectra from polar molecules

The energy level of photons in terahertz band is about 1–10 meV, which is the same as the molecular transition. Therefore, THz radiation is able to probe intermolecular and intramolecular interactions of complex molecules, and many polar molecules exhibit unique spectral signatures in this region, arising from transitions between the rotational states [19–21]. Once THz wave spectroscopy is measured, one can identify those resonant energy levels through the absorption peaks. In our experiments, when laser pulses ionize the gas medium in chamber, some new polar molecules can be generated. For example, in the case of CO_2, CO and O_3 as the main products of ionization and also the polar molecules will induce many absorption peaks in the THz spectrum (see Fig. 3a). Similarly, in the case of O_2, O_3 also exists as the main product of ionization and induces the same absorption peak at 0.9 THz, as shown in Fig. 3b. Furthermore, their experimental results show that the absorption peaks are much wider as the usual case [22, 23]. We presume that the complicated mixtures of ions and molecules make their absorption spectra overlap with each other; as a result, we can only see the spectrum with wide absorption peaks and their amplitude fluctuation. On the contrary, Ar and N_2, including their ionization products (see Table 1), are all nonpolar molecules, which determines they are all transparent in this terahertz range, and then no specific absorption peaks can be formed.

2. Vibrational spectra from intermolecular interactions

For the intermolecular interactions, the charge carried by different atoms will affect their absorption spectra. Here, the charges carried by atoms in each molecule are listed in Table 2. It can be seen that, for CO_2, CO, O_3 molecules, their atoms carry charges, which can affect intermolecular interactions and then may induce new THz absorption. Certainly, considering the gas density is much smaller than that of solid and liquid, the corresponding absorption will be much smaller. While for O_2, Ar and N_2 (their atoms barely carry charges), there should be almost no vibrational interactions between molecules or the vibrational behavior of combinations of bonds, and then no contributions for the THz absorption spectrum. Besides, considering the water vapor is little in the gas chamber, the vibrational features associated

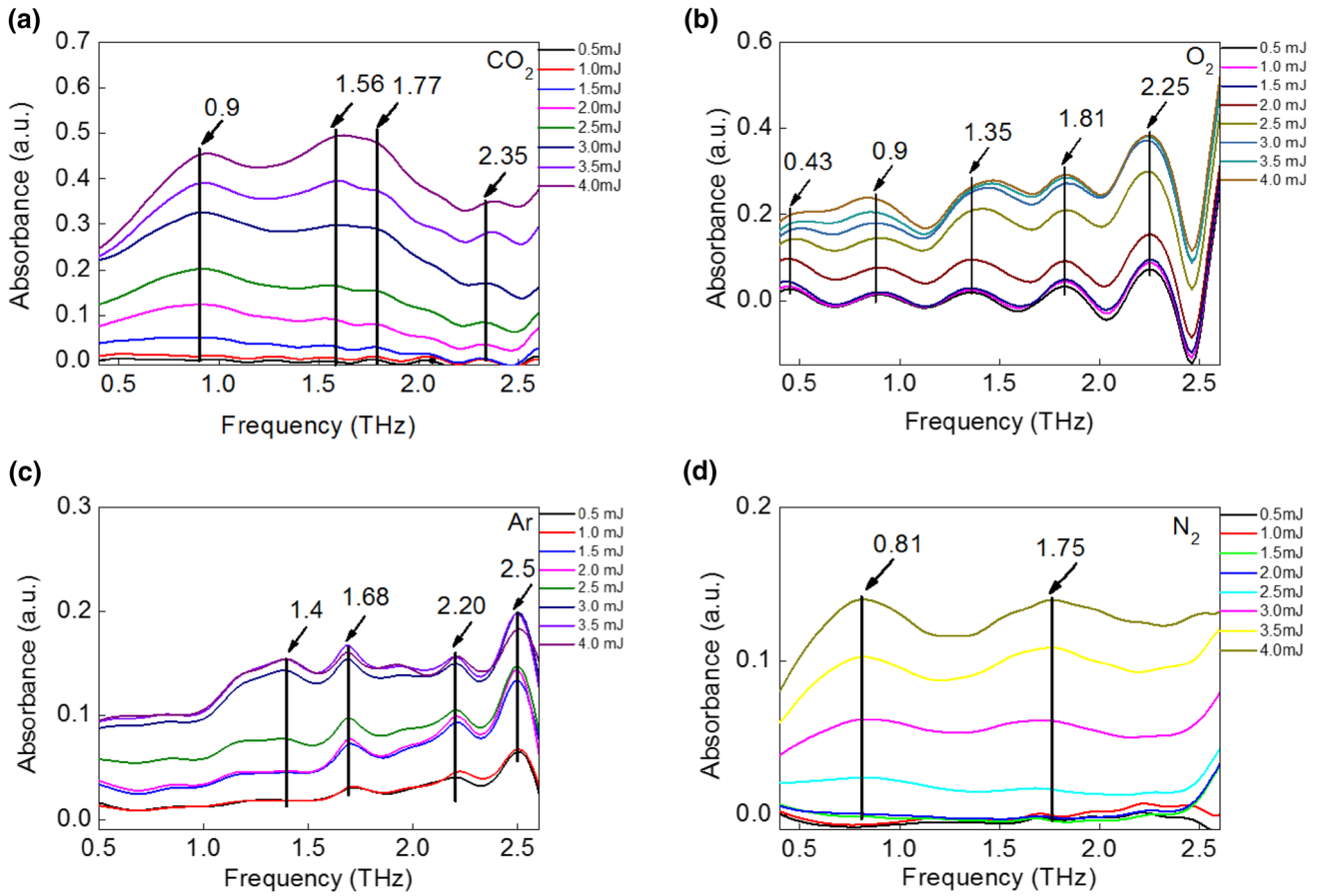

Fig. 3 Absorbance of THz wave under different pump energies for plasma sheet formed in the gas environment of **a** CO_2 **b** O_2 **c** Ar and **d** N_2. Pump energies for the formation of plasma sheet are labeled on each figure. The corresponding THz absorption peaks are also labeled

Table 1 The initial gases and their products of ionization

Molecule	Products of ionization		
	Positive ions	Negative ions	Neutral molecules/atoms
CO_2	CO_2^+, CO^+, O_2^+, O^+, C^+	e	CO, O_2, O_3
O_2	O_2^+, O^+, O^{2+}	e	O_3, O
Ar	Ar^+	e	/
N_2	N^+, N^{2+}, N_4^+	e	N

Table 2 The initial gases and their products of ionization

Molecule	Atom	Charge (e)
CO_2 [24]	C	+0.544
	O	−0.272
CO [24]	C	+0.107
	O	−0.107
O_2 [25]	O	0
O_3 [26]	O_{center}	+0.12
	O_{side}	−0.06
Ar [27]	Ar	0
N_2 [28]	N	0

with intermolecular hydrogen bond relative motions can be neglected.

3. Collision-induced absorption and spectral broadening

In the region of plasma sheet, the collision between atoms, molecules, ions and electrons is unavoidable. Usually, collision behavior caused by Lorentz force is generally small in the presence of low energy electromagnetic waves as THz wave. However, in our case, the strongly focused femtosecond laser pulses (peak intensity $> 10^{14}$ W/cm^2) greatly increases the temperature in the plasma (several hundred to several thousand Kelvin degrees [29]) and then enhances the collision behavior between particles. These collision behaviors can further cause the electrons at a low energy level to leap to a higher energy state, supported by the energy provided by absorbing the THz wave [30]. Additionally, the existing absorption peaks will also be strongly broadened due to the reason of collisional dephasing [31],

as shown in Fig. 1. Here, considering the non-polarity and electric neutrality of Ar and N_2, we deduce that the collision-induced absorption is the main reason for their spectral characteristics. Interestingly, we note that the spectra in the case of N_2 measured at low THz energy (< 2.0 mJ) are inconsistent with those measured at high energy (> 2.5 mJ) (see Fig. 3d), i.e., the 0.81 THz absorption peak only formed when the pump energy for the formation of plasma sheet reaches a threshold. We believe this threshold corresponding to the ionization of N_2 progresses to the ionization of N_2^+, determined by the different pump laser intensities. Specifically, at low pump intensity, only the initial N_2 molecules are ionized; when the laser intensity increases to a threshold, the N_2^+ become the main medium and then be further ionized, which leads to the slightly different absorption spectrum. Here, considering the spectrum is contributed by many reasons, therefore, we can only give the qualitative analysis. The further quantitative analyses may be investigated in the future.

4 Conclusion

Basing on the laser plasma sheet and terahertz spectroscopy, we experimentally investigate the THz absorption spectrum of plasma sheet formed in different gas mediums (CO_2, O_2, Ar and N_2). It is found that as the pump energy of plasma sheet increases, the absorbance of THz wave presents strong dependence on the gas kind, i.e., the plasma formed in different gas mediums caused different absorption peaks. The reasons for these absorption peaks are related to the molecular polarity, electric charge, intermolecular and intramolecular interactions, and collisional absorption of gas molecules. These results are meaningful for promoting the development of gas remote sensing and the application of broadband terahertz wave.

Acknowledgements The authors are grateful to Professor Yi Liu and Bo Song for fruitful discussions. This work is financially supported by Major National Development Project of Scientific Instrument and Equipment (2017YFF0106300), NSFC (61771314), Shanghai Rising-Star Program (17QA1402500), Shuguang Program (17SG45), Shanghai Pujiang Program (16PJD033), and Young Yangtse Rive Scholar (Q2016212).

References

1. M. Rodriguez, R. Bourayou, G. Méjean, J. Kasparian, J. Yu, E. Salmon, A. Scholz, B. Stecklum, J. Eislöffel, U. Laux, A.P. Hatzes, R. Sauerbrey, L. Wöste, J. Wolf, Phys. Rev. E **69**, 036607 (2004)
2. S.L. Chin, S.A. Hosseini, W. Liu, Q. Luo, F. Théberge, N. Aközbek, A. Becker, V.P. Kandidov, O.G. Kosareva, H. Schroeder, Can. J. Phys. **83**, 863 (2005)
3. P. Sprangle, J.R. Peñano, B. Hafizi, Phys. Rev. E **66**, 046418 (2002)
4. Z. Mics, F. Kadlec, P. Kužela, P. Jungwirth, S.E. Bradforth, V.A. Apkarian, J. Chem. Phys. **123**, 104310 (2005)
5. S.P. Jamison, J. Shen, D.R. Jones, R.C. Issac, B. Ersfeld, D. Clark, D.A. Jaroszynsky, J. Appl. Phys. **93**, 4334 (2003)
6. M. Kress, T. Löffler, S. Eden, M. Thomson, H.G. Roskos, Opt. Lett. **29**, 1120 (2004)
7. D.R. Thompson, D.C. Benner, L.R. Brown, D. Crisp, V.M. Devi, Y.B. Jiang et al., J. Quant. Spectr. Rad. Transf. **113**, 2265 (2012)
8. M. Yokomizo, Fujitsu Sci.Tech. **44**, 410 (2008)
9. A.V. Nikitin, O.M. Lyulin, S.N. Mikhailenko, V.I. Perevalov, N.N. Filippov, I.M. Grigoriev, et al., J. Quant. Spectr. Rad. Transf. **111**, 2211 (2010)
10. B. Bézard, A. Fedorova, J.L. Bertaux, A. Rodin, O. Korablev, Icarus **216**, 173 (2011)
11. M.J. Frisch, G.W. Trucks, H.B. Schlegel et al., *Gaussian 09, Revision A. 01*. (Gaussian, Wallingford, 2009)
12. A. Couairona, A. Mysyrowicz, Phys. Rep. **441**, 47 (2007)
13. L. Berge et al., Rep. Prog. Phys. **70**, 1633 (2007)
14. K. Kim, J.H. Glownia, A.J. Taylor, G. Rodriguez, IEEE J. Quantum Electron. **48**, 797 (2012)
15. W. Wang, Y. Li, Z. Sheng, X. Lu, J. Zhang, Phys. Rev. E **87**, 033108 (2013)
16. H. Thom, Dunning, Jr., Highlights in theoretical chemistry. Theor. Chem. Acc. **134**, 1 (2015)
17. V.A. Andreeva et al., Phys. Rev L **116.6**, 063902 (2016)
18. L. Bergé et al., Phys. Rev L **110.7**, 073901 (2013)
19. R.H. Jacobsen, D.M. Mittleman, M.C. Nuss, Opt. Lett. **21**(24), 2011 (1996)
20. D. Woolard, R. Kaul, R. Suenram, A.H. Walker, T. Globus, A. Samuels, in IEEE MTT-S Int. Microwave Symp. Dig. Anaheim, CA, pp. 925–928, (1999)
21. F.C. De Lucia, in ed. by D Mittleman *Sensing with Terahertz Radiation* (Springer, Berlin, 2003)
22. Z. Mics, F. Kadlec, P. Kužel et al., J. Chem. Phys. **123**, 104310 (2005)
23. Y. Peng, X. Yuan, X. Zou, W. Chen, H. Huang, H. Zhao, L. Chen, Y. Zhu, Biomed. Opt. Express **7**, 4472 (2016)
24. A. Sirjoosingh, S. Alavi, T.K. Woo, J. Phys. Chem. C **114**, 2171 (2010)
25. J. Yang, Y. Ren, A. Tian et al., J. Phys. Chem. B **104**, 4951 (2000)
26. M. Roeselova, P. Jungwirth, D.J. Tobias et al., J. Phys. Chem. B **107**, 12690 (2003)
27. L. Verlet, J.J. Weis, Mol. Phys. **24**, 1013 (1972)
28. M. Zhang, G. Zuo, J. Chen et al., Sci. Rep. **3**, 1660 (2013)
29. G. Point, E. Thouin, A. Mysyrowicz, A. Houard, Opt. Express **24**, 6271 (2016)
30. J. Zhao, L.L. Zhang, T. Wu et al., Opt. Commun. **380**, 87 (2016)
31. H. Harde, R.A. Cheville, D. Grischkowsky, J. Phys. Chem. A **101**, 3646 (1997)